Dynamic Performance Analysis of an Inverter-Based PV Plant during Sunrise and Sunsets through Synchrophasors

Bikal Pudasaini
Dominion Energy, Inc.
Richmond, VA, USA
bikal.pudasaini@dominionenergy.com

Luigi Vanfretti
ECSE Department
Rensselaer Polytechnic Institute
Troy, NY, USA

Chetan Mishra, Jaime De La Ree Jr., Kevin D Jones
Dominion Energy, Inc.
Richmond, VA, USA

***Abstract*—In recent years, inverter-based photovoltaic (PV) plants have become an important part of the modern power grid. In addition to supplying clean energy, they help regulate voltage and maintain the power factor at the point of interconnection. However, the complex behavior of these inverter-based resources (IBR) can sometimes lead to false alarms in modal estimation or oscillation detection tools. In turn, this brings new situational awareness challenges to power system operators, who need to discern between such complex IBR responses and conventional grid dynamics and determine how to address each type of behavior when they occur at lower frequencies. This paper analyzes one type of dynamic behavior from a PV plant at Dominion Energy, which was reported as an oscillation although, as shown in this study, it was actually a nonlinear response result of the plant control mechanism. Using ambient synchrophasor data and a detailed review of the plant's controller and inverter configuration, we provide a root cause analysis to better understand the factors behind this complex dynamic behavior.**

***Index Terms*— Inverter-based PV Plant, IBR dynamic performance, power plant controller, spectral analysis, synchrophasor, PMU**

I. INTRODUCTION

The increasing adoption of renewable energy, particularly wind and solar photovoltaic (PV) systems, is transforming the way electricity is generated and delivered. Photovoltaic energy is integrated through inverters, which serve as an interface between fluctuating energy supply and the power grid. Unlike conventional power plants based-on synchronous machines, such kind of inverter-based resources (IBRs) behave differently and can present more complex dynamics due to nonlinear interactions with the grid and sensitivity to changes in the power system. With changing conditions in solar radiation and wind speeds, it is difficult to predict and manage the performance of IBR-based systems including PV plants [1]. Synchrophasor measurements have become an essential tool for gaining a deeper understanding of how IBRs perform, helping to understand and mitigate potential stability issues [2, 3].

Spectral analysis applied to synchrophasor measurements provides valuable information of lightly damped low frequency modes in power systems. For this purpose, synchrophasor-based software tools are used by power system operators to track important inter-area modes and detect electromechanical oscillations in the system [4, 5]. However, various nonlinear dynamic behaviors in the system may affect the performance of these analysis. For instance, in [6] and [7], the challenges of ambient-mode estimation and damping estimation in the presence of forced oscillation are presented, which indicate the need of understanding and analysis of such behaviors when using methods and tools for ambient synchrophasor data analysis.

Both mode estimators or oscillation detection tools [8] may be triggered from different dynamic behaviors of IBRs, in fact, some of these tools have been exploited to detect interactions between wind farms and the grid [9]. This poses a challenge for oscillation monitoring tools that have been put in place to monitor conventional grid dynamics [5]. This is due to the fact that if the estimated frequency lies in the lower frequency range of the inter-area or local modes, a false alarm may be raised or mode estimates can be corrupted [6, 7]. In turn, system operators may face decision and situational awareness challenges to adequately address and mitigate these behaviors. In this paper, we analyze one of such numerous dynamics that could be seen in IBRs using ambient synchrophasor measurements. In this study case, the operators got an alarm of an oscillation in the [0, 0.15] Hz frequency range from a pre-configured oscillation monitoring tool. However, after detailed analysis, it was determined that the alarm was activated not from the excitation of an inter-area mode (which typically arise at this range), but instead from a PV plant connected to the 115 kV transmission system in Dominion Energy. This paper provides an analysis of the PV plant's response that explains why the alarm from the oscillation monitoring tool was activated, and moreover, how a nonlinear response such as the one described can be perceived as an oscillation when using such tools. This work helps operators and engineers build awareness about the need to carefully consider notifications and alarms generated by detection tools, especially with the large integration of IBRs with complex behaviors.

The reminder of this paper is organized as follows. In Section II, information of the PV plant under study is provided along with measurement device specifications. Section III presents the necessary but brief theoretical background needed to understand methods used in ambient data analysis. Section IV gives details of the analysis and results obtained. This includes characterization of the behavior under study and root cause of the underlying phenomenon. Section V concludes the paper.

II. DETAILS

A. Plant Specfications

The PV plant under study has an output capacity of 105 MW and consists of 42 photovoltaic inverters (2500 kW / 2700 kVA each). The inverters operate at an inverter voltage of 600 VAC nominal, connected via forty-two 2.5 MVA, 600 V/34.5 kV (LV/MV) unit step-up transformers. These transformers are grouped into 4 individual collectors, that make 2 groups of feeders (20 transformers to first feeder and 22 to second feeder). These two feeders are connected to the plant substation. The plant substation 34.5 kV bus is also equipped with a capacitor bank of 12.5 MVAR to supply reactive power to the grid as required. From there, a 34.5 kV/115 kV (MV/HV) main generation step-up transformer (GSUT) connects the facility to the 34.5 kV/115 kV transmission system at a transmission substation, serving as the point of interconnection (POI). A simplified diagram of the plant is shown in Fig. 1.

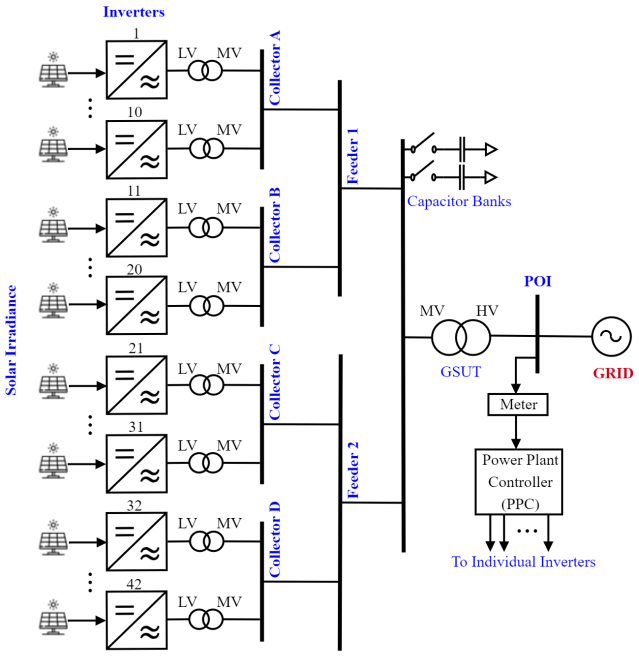

Fig. 1. Simplified diagram of grid-connected PV plant under study.

B. Power Plant Controller

In the plant under study, as shown in Fig. 1, Power Plant Controller (PPC)'s provides functions to manage the voltage and the power factor at the generation facility's POI. This is done by continuously monitoring the POI voltage and power factor (PF), and automatically adjusting the reactive power (VARs) capabilities of the inverters and capacitor banks as needed to meet the POI voltage and PF requirements.

The control functions of the PPC aim to regulate the voltage and power factor at the PO, at which two specifications need to be respected:

1. *PF limit:* The PF limit is a specified percentage value that is used to restrict the PPC from operating the plant too far from unity. The limit is used for both leading and lagging PF limits. The value set is 5%, which translates to limiting the plant response to maintain a PF from 0.95 lagging to 0.95 leading as measured at the POI.
2. *Voltage limit:* The % voltage limit is a number that is used to restrict the POI voltage and is used as both over and under voltage limits. The set value is 5% and this limit will allow the PPC to operate the plant +5%/-5% of the utility rated voltage.

C. Measurement Data

Dominion Energy has synchrophasor measurements visibility across the majority of its transmission network through its fleet of Digital Fault Recorders (DFR), which include PMU functionalities. The sampling rate of a DFR is 4800 Hz. The 4800 Hz signal is down sampled to 960 Hz from which a 30 Hz phasor component is reported. The data is stored and can be accessed through the cloud-based PredictiveGrid™ platform. In this work the 30 Hz reported phasors are used.

III. THEORETICAL BACKGROUND

This section provides a brief description of the spectral analysis methods used in this work [10]. The methods were implemented in Python and use the SciPy library.

A. Power Spectral Density (PSD)

The power spectral density (PSD) of a signal describes the distribution of power over frequency. For a discrete time signal $y(t)$ at a frequency f, the PSD is given as,

$$\phi(f) = \sum_{k=-\infty}^{\infty} r(k)\, e^{-i2\pi fk} \tag{1}$$

where $r(k)$ is the autocovariance sequence of $y(t)$, given by

$$r(k) = E\{y(t)y^*(t-k)\} \tag{2}$$

where $E\{.\}$ denotes the expectation operator, which averages over the ensemble of realizations. For a finite sampled data window of length N, the PSD can be written as:

$$\phi(f) = \lim_{N\to\infty} E\left\{\frac{1}{N}\left|\sum_{n=0}^{N-1} y(n)e^{\frac{-i2\pi fn}{N}}\right|^2\right\}. \tag{3}$$

To obtain a low variance estimate of the PSD, Welch's method [11] is used, which can be summarized as follows:

1. The data window is divided into N_b overlapping block intervals of length N_t.
2. Each block is convolved with a window function $w(n)$ to obtain a new signal $w * y$.
3. PSD for each interval is estimated as follows:

$$\hat{\phi}(f,m) = \frac{1}{N_t}\left|\sum_{n=m}^{m+N_t-1} (y*w)(n)e^{\frac{-i2\pi fn}{N_t}}\right|^2 \tag{4}$$

4. The PSD estimates above are averaged to obtain the final estimates:

$$\hat{\phi}(f) = \sum_{m=0}^{N_b-1} \hat{\phi}(f,m). \quad (5)$$

In this paper, a window length of 20 minutes is used, with overlapping blocks of 2 minutes and a 50% overlap between successive blocks. The window function employed is Hanning.

B. Spectrogram

A spectrogram is a visual representation of the spectrum of frequencies of a signal over time and is one of the preferred tools for time-frequency analysis. This method helps to uncover persistent dynamic behaviors or modes within the system. In this paper, a Short Time Fourier Transform (STFT)-based spectrogram is utilized. For a signal y, the STFT provides the time-frequency coefficients Y as follows:

$$Y(f,m) = \sum_{n}^{N-1} y(n)w(n-m)e^{\frac{-i2\pi fn}{N}} \quad (4)$$

where $w(n)$ is a window function. The time-varying spectrum, $\phi(f,m) = |Y(f,m)|^2$ is visually represented in the spectrogram. In this paper, the window length of 2 minutes with a 50% overlap between successive windows is used.

IV. Analysis and Results

A. First observation

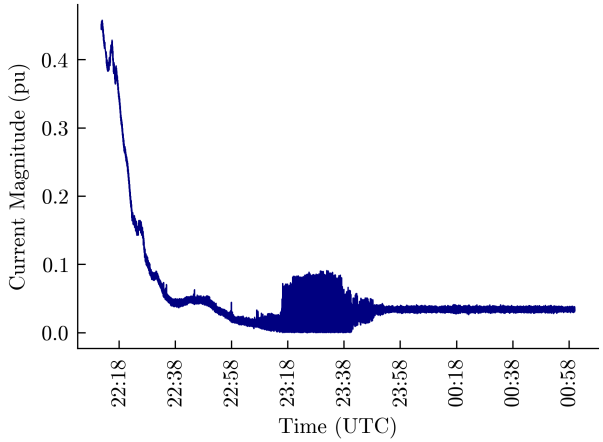

Fig. 2. Current magnitude signal at the output of the solar plant during the low active power generation period around sunset time on May 4, 2024.

The main behavior addressed in this paper was first reported on May 4, 2024, commencing at approximately 11:15 PM (UTC) and persisting for about 40 minutes. It was reported as an alarm configured in an oscillation detection tool in use at Dominion Energy. The application continuously monitors the PSD of multiple signals from PMUs across various frequency ranges and generates an alarm if the PSD exceeds predefined thresholds. In this case, the frequency range was [0, 0.15] Hz. From here onwards, we will call it the *'perceived oscillation'*. Fig. 2 shows a snapshot of the measured plant current magnitude when the perceived oscillation was reported. It is important to note that the current injection from the PV plant was measured at the higher side of the transformer at the POI, consequently, it is comprised of the individual response of 42 inverters within the plant. This period coincides with the sunset, during which the power generation of the plant is minimal due to low solar irradiance. Observe that during this period, current from the plant decreases and approaches zero.

B. Frequency Domain Characterization

Proper characterization in the frequency-domain is crucial for understanding the plant's dynamic behavior. A 20-minute window (from 11:20 PM to 11:40 PM (UTC)) of the current magnitude signal (Fig. 2) was analyzed. This signal was used to calculate the PSD using Welch's method, as discussed in Section III.A. Fig. 3 illustrates the PSD up to 1 Hz, highlighting the frequency at which the signal exhibits the highest power. The red dashed horizontal line shows the approximate predefined threshold value that raised the alarm of the perceived oscillation in the [0, 0.15] Hz frequency range. Although the peak with the highest magnitude of PSD occurs at a lower frequency, numerous peaks are observed at higher frequencies as well. A closer examination of the PSD reveals how these peaks reveal themselves as harmonic components of the perceived oscillation frequency, which is around 0.07 Hz. This kind of frequency response is typical of non-linear behavior that emerges from a non-sinusoidal time-domain response (see [12] for a similar type of response).

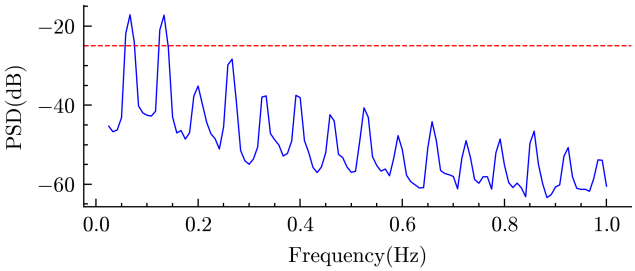

Fig. 3. PSD of the current magnitude signal at the output of the solar plant during the perceived oscillation, revealing multiple peaks.

C. Long-term trend using spectrogram

Following the first observed oscillation during sunset, this section investigates the event's potential long term trends using time-frequency analysis, captures the dynamic behaviors over an extended timeframe and identify any recurring patterns that are not apparent from single-instance observations.

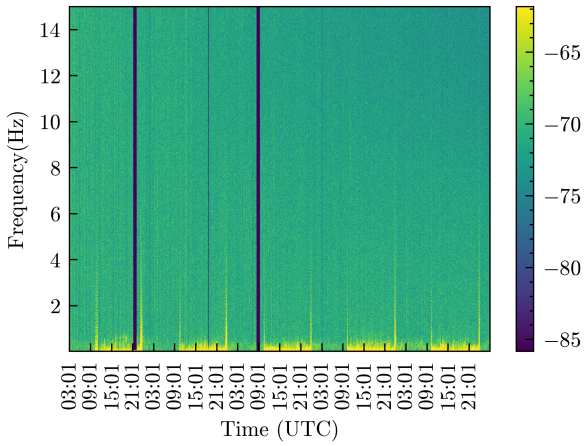

Fig. 4. Spectrogram of the current magnitude signal at the output of the solar plant for five consecutive days starting at 3 AM (UTC) on May 4, 2024.

Fig. 4 shows the spectrogram of the current magnitude signal at the solar plant's output over five consecutive days, beginning at 3 AM (UTC) on May 4, 2024. The spectrogram was calculated using the STFT-based method discussed in III.B. A consistent pattern emerges, showing that the perceived oscillation recurs daily during sunrise and sunset intervals, as shown by yellow spikes corresponding to higher signal power. This behavior coincides with periods of reduced active power output from the solar plant, suggesting a potential relationship between low power output conditions and the initiation of these behaviors.

An additional spectrogram is plotted focusing on a lower frequency range of 0 to 0.5 Hz, as shown in Fig. 5. This captures the harmonic components of the observed oscillations, like those identified in Section III.B's single-incident analysis. The analysis confirms the presence of the same dynamic behavior across multiple days and under similar conditions, i.e. during the periods of low active power output at sunrise and sunset. In fact, these behaviors are not limited to the five days observed; they have been consistently seen every morning and evening up to the present day. The two instances of dark blue vertical stripes across the full spectrum in Fig. 4 and Fig. 5 represent missing data in the signal.

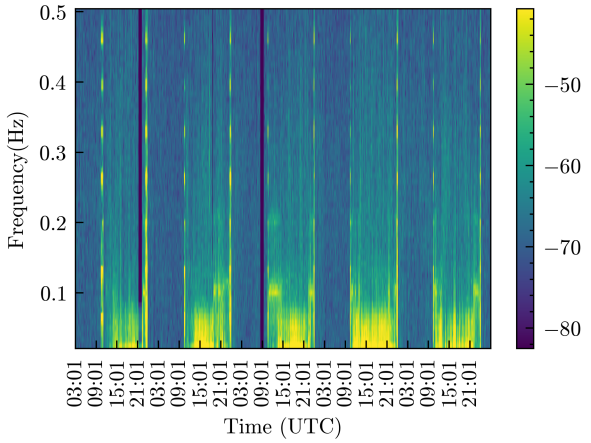

Fig. 5. Spectrogram of the current magnitude signal at the output of the solar plant at a lower frequency range for five consecutive days starting at 3 AM (UTC) on May 4, 2024.

D. Root Cause Analysis of the Underlying Phenomenon

Fig. 6 presents the active power, reactive power, and power factor plots at the PV plant's output, beginning a few hours before sunset. Three immediate observations can be made as follows:

1. The perceived oscillation is only seen by the reactive power signal but not active power.
2. Before the output active power starts ramping down (left side of dashed vertical black lines), the plant can maintain the PF between 1 and 0.95. This aligns to the PPC settings we detailed for PF in Section II. B, i.e. the PF limit will allow the PPC to operate the plant from 0.95 lagging to 0.95 leading.
3. As the active power output decreases, the PF gradually worsens from the 0.95 limit (dashed horizontal pink line). The PPC is a slow controller and is also affected by communication time-delays. The PF deviation during these ramp downs is likely due to these delays between the PPC control and inverter control as observed in [3].
4. The large fluctuations in reactive power are observed when the active power output nears zero, which we are interested in.

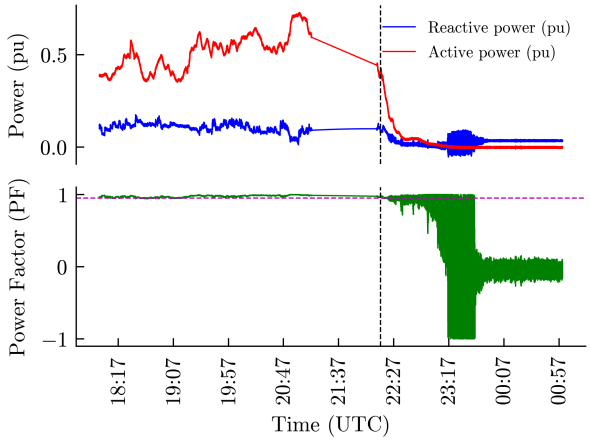

Fig. 6. Active power, reactive power and power factor plot at the output of the solar plant beginning a few hours before sunset time on May 4, 2024.

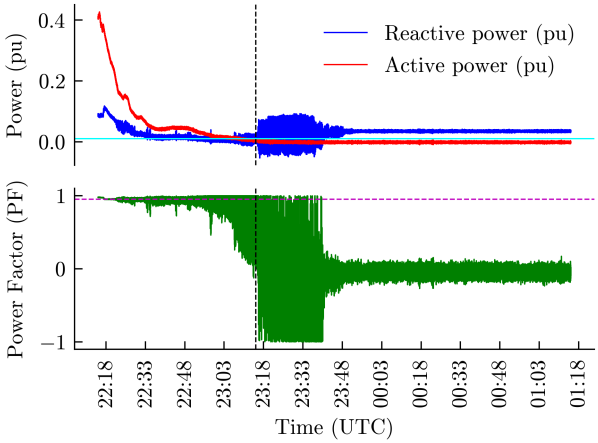

Fig. 7. Active power, reactive power and power factor plot at the output of the solar plant around sunset time on May 4, 2024.

The reported dynamic behavior or the perceived oscillation starts around 11.15 PM (UTC), i.e., right side of the vertical dashed black line shown in Fig. 7. The cyan horizontal shows an approximate active power threshold of 1 MW or 0.01 pu, below which significant reactive power fluctuations are observed, that helps us understand the underlying mechanism of the behavior. Furthermore, an analysis of the PPC/inverter commissioning documentation, manuals, and other documentation helped to develop the following insights and understandings:

1. PPC: If MW production falls below 1 MW, the PCC voltage control function is disabled and a (0) MVAR setpoint is sent to all (42) inverters.
2. Inverters: If each inverter's $V_{dc} < 860\,V$ or $P_{in} < 22\,kW$, the inverter goes from Maximum Power Point Tracking (MPPT) mode to grid-connected stand-by

mode, where the inverter stops switching, but is connected to the grid. We have 42 inverters in the plant, and $42 \times 22 = 924\ kW$, which is close to 1 MW. This is possibly the motivation for disabling PPC voltage control function below 1 MW output since some or all inverters might be switched off.

3. Inverters: The accuracy of reactive power and PF measurements drops when the dc power is small, as indicated by the inverter manufacturer.

Fig. 8 shows the first five minutes of large fluctuations in the reactive power. During this period, the active power output fluctuates between small positive and negative values. The small positive output is expected due to insufficient irradiance. When inverters are off, negative active power values arise from reverse power flow from the grid, needed to energize equipment such as transformers and cables. This occurs due to a change in current flow direction measured at the PPC, as the current reverses at the PCC and flows into the plant when there is insufficient power to maintain the feeders energized. This results in a reversal of the power factor being measured, and consequently, the control target imposed by the PF limit specifications of the PCC controller.

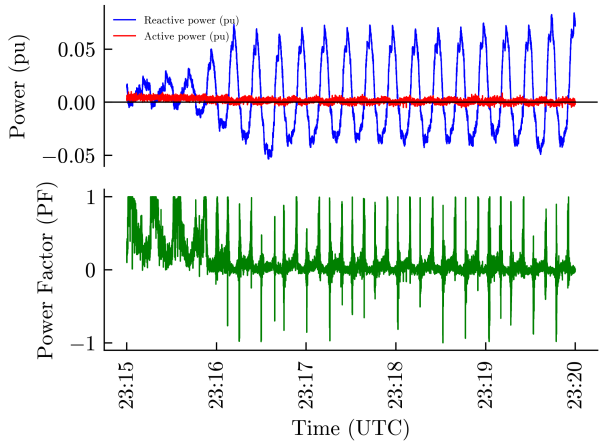

Fig. 8. Active power, reactive power and power factor plot at the output of the solar plant during the initiation of reactive power fluctuations.

From the power factor plot in Fig. 8, we can observe that the inverter attempts to maintain the PF within the (0.95, 1) range during periods of positive active power output by increasing reactive power and targets the (-0.95, -1) range during negative active power output by decreasing the reactive power, producing this nonlinear dynamic response. This misled the alarming threshold of the oscillation detection application as it is *perceived* as a low-frequency oscillation at the typical range of inter-area modes. Although PPC voltage control function is disabled and (0) MVAR setpoint is sent to all the inverters when MW output falls below 1 MW, the inverters still produce MVAR in an attempt to maintain the power factor within limits but fail to do so. This manifests as the demonstrated nonlinear dynamic behavior.

This unforeseen dynamic behavior has been observed in IBR-based resources at Dominion Energy, alongside behaviors noted in [3, 4]. Operators should be careful when responding to alarms from the oscillation detection application, as they are based signal's PSD and are not selective for oscillations. Addressing such undesirable responses will require strategic coordination between the PPC and inverters to enhance performance and stability, presenting a valuable topic for further research.

V. Conclusions

This paper analyzes an undesired and unforeseen nonlinear dynamic behavior at a 105 MW IBR-based PV plant interconnected with Dominion Energy's system. Initially detected by oscillation detection software, the analysis reveals that this perceived oscillation stems from the nonlinear interaction between the PV plant's controller and its 42 inverters during sunrise and sunset. The long-term trend of the identified dynamics was analyzed to better understand the cause of this unusual behavior, which appeared consistently during sunrise and sunset when the active power output was low. Ultimately, the root cause of this undesirable behavior was the inverters' struggle to maintain the power factor within limits during low active power output.

References

[1] B. Kroposki *et al.*, "Achieving a 100% Renewable Grid: Operating Electric Power Systems with Extremely High Levels of Variable Renewable Energy," in *IEEE Power and Energy Magazine*, vol. 15, no. 2, pp. 61-73, March-April 2017, doi: 10.1109/MPE.2016.2637122.

[2] C. Mishra, L. Vanfretti, J. Delaree and K. D. Jones, "Analyzing a Non-Sinusoidal Response from a Real-World Solar PV," in *IEEE Transactions on Power Systems*, vol. 39, no. 2, pp. 4771-4774, March 2024, doi: 10.1109/TPWRS.2024.3350377.

[3] C. Wang, C. Mishra, K. D. Jones, R. M. Gardner and L. Vanfretti, "Identifying Oscillations Injected by Inverter-Based Solar Energy Sources," *2022 IEEE Power & Energy Society General Meeting (PESGM)*, Denver, CO, USA, 2022, pp. 1-5, doi: 10.1109/PESGM48719.2022.9916830.

[4] G. Rogers, Power System Oscillations, Kluwer Academic Publishers, 1999.

[5] J. F. Hauer, D. J. Trudnowski and J. G. DeSteese, "A Perspective on WAMS Analysis Tools for Tracking of Oscillatory Dynamics," 2007 IEEE Power Engineering Society General Meeting, Tampa, FL, USA, 2007, pp. 1-10, doi: 10.1109/PES.2007.386186.

[6] V. S. Perić and L. Vanfretti, "Power-System Ambient-Mode Estimation Considering Spectral Load Properties," in *IEEE Transactions on Power Systems*, vol. 29, no. 3, pp. 1133-1143, May 2014, doi: 10.1109/TPWRS.2013.2292331.

[7] L. Vanfretti, S. Bengtsson, V. S. Perić and J. O. Gjerde, "Effects of forced oscillations in power system damping estimation," *2012 IEEE International Workshop on Applied Measurements for Power Systems (AMPS) Proceedings*, Aachen, Germany, 2012, pp. 1-6, doi: 10.1109/AMPS.2012.6344015.

[8] J. F. Hauer and F. Vakili, "An oscillation detector used in the BPA power system disturbance monitor," in *IEEE Transactions on Power Systems*, vol. 5, no. 1, pp. 74-79, Feb. 1990, doi: 10.1109/59.49089.

[9] L. Vanfretti, M. Baudette, J.L. Dominguez-Garcia, M.S. Almas, A. White, and J.O. Gjerde, "A PMU-Based Real-Time Oscillation Detection Application for Monitoring Wind-Farm Dynamics," *Electric Power Components and Systems, Taylor & Francis,* Vol. 44, Iss. 2, 2016. http://dx.doi.org/10.1080/15325008.2015.1101727

[10] P. Stoica and R.L. Moses, *Spectral Analysis of Signals*. Upper Saddle River, NJ, USA: Pearson/Prentice Hall, 2005.

[11] P. Welch, "The use of fast Fourier transform for the estimation of power spectra: A method based on time averaging over short, modified periodograms," in *IEEE Transactions on Audio and Electroacoustics*, vol. 15, no. 2, pp. 70-73, June 1967, doi: 10.1109/TAU.1967.1161901

[12] X. Xu *et al.*, "Tracking Periodic Voltage Sags via Synchrophasor Data in a Geographically Bounded Service Territory," *2023 IEEE PES Grid Edge Technologies Conference & Exposition (Grid Edge)*, San Diego, CA, USA, 2023, pp. 1-5, doi: 10.1109/GridEdge54130.2023.10102706.1